Journal of Theoretical Biology 407 (2016) 198–211

Contents lists available at ScienceDirect

Journal of Theoretical Biology

journal homepage: www.elsevier.com/locate/yjtbi

Somatic Growth Dilution of a toxicant in a predator–prey model under stoichiometric constraints

Angela Peace [a,b,*], Monica D. Poteat [c], Hao Wang [d]

[a] Department of Mathematics and Statistics, Texas Tech University, Lubbock, USA
[b] National Institute for Mathematical and Biological Synthesis, University of Tennessee, USA
[c] Environmental Sciences Division, Oak Ridge National Laboratory, Oak Ridge, TN, USA
[d] Centre for Mathematical Biology, Department of Mathematical and Statistical Sciences, University of Alberta, Edmonton, AB, Canada T6G 2G1

HIGHLIGHTS

- We integrated realistic ecological processes into an aquatic ecotoxicology model.
- Stoichiometric predator–prey model parameterized to Algae–Daphnia subject to MeHg.
- The ODE model investigates concurrent nutrient and toxicant stressors.
- Analytical analysis, numerical simulations, bifurcation analysis are performed.
- The model captures and explores the Somatic Growth Dilution phenomenon.

ARTICLE INFO

Article history:
Received 16 March 2016
Received in revised form
9 June 2016
Accepted 21 July 2016
Available online 25 July 2016

Keywords:
Methylmercury
Predator–prey model
Ecological stoichiometry
Ecotoxicology

ABSTRACT

The development of aquatic food chain models that incorporate both the effects of nutrient availability, as well as, track toxicants through trophic levels will shed light on ecotoxicological processes and ultimately help improve risk assessment efforts. Here we develop a stoichiometric aquatic food chain model of two trophic levels that investigates concurrent nutrient and toxic stressors in order to improve our understanding of the processes governing the trophic transfer for nutrients, energy, and toxicants. Analytical analysis of positive invariance, local stability of boundary equilibria, numerical simulations, and bifurcation analysis are presented. The model captures and explores a phenomenon called the Somatic Growth Dilution (SGD) effect recently observed empirically, where organisms experience a greater than proportional gain in biomass relative to toxicant concentrations when consuming food with high nutritional content vs. low quality food.

1. Introduction

Chemical contaminants are widely dispersed throughout Earth's ecosystems due to a multitude of human activities, as well as natural phenomena, and have the potential to adversely impact a diverse range of organisms (Walker et al., 2012). Bioaccumulation of toxic compounds in aquatic food chains can pose risk to ecosystem conservation as well as wildlife and human health. Accurately assessing the risks of contaminants requires more than an understanding of the effects of contaminants on individual organisms, but requires further understandings of complex ecological interactions, elemental cycling, and the interactive effects of natural stressors, such as resource limitations, and contaminant stressors.

Ecotoxicological modeling aims to predict how contaminants cycle through aquatic food systems. It is vital to understand the processes that determine the trophic transfer of toxicants to improve developed risk assessment protocols. Wang et al. (1996) developed a simple biokinetic model that has been used to predict total bioaccumulated toxicant concentrations in multiple species of aquatic organisms over that last decade (Wang and Rainbow, 2008; Wang, 2012). It models the change in toxicant concentration (v) in an organism due to uptake and loss due to efflux and growth:

$$\underbrace{\frac{dv}{dt}}_{\substack{\text{Change in toxicant conc.}\\ \text{of predator over time}}} = \underbrace{a_2 T}_{\substack{\text{uptake from}\\ \text{water}}} + \underbrace{\xi f u}_{\substack{\text{uptake from}\\ \text{consuming prey}}} - \underbrace{(\sigma_2 + g)v}_{\substack{\text{loss due to}\\ \text{efflux \& growth}}} \tag{1}$$

* Corresponding author at: Department of Mathematics and Statistics, Texas Tech University, Lubbock, USA.
E-mail address: a.peace@ttu.edu (A. Peace).

http://dx.doi.org/10.1016/j.jtbi.2016.07.036
0022-5193/

where a_2 is the uptake rate constant from the dissolved toxicant, T is the concentration of dissolved toxicant, ξ is the toxicant assimilation efficiency, f is the predator's ingestion rate, u is the toxicant concentration in the prey, σ_2 is the toxicant efflux rate, and g is the predator's growth rate. The Biokinetic model (1) incorporates constant parameters for the predator's growth rate (g) and ingestion rate (f). It also assumes the quantity and toxicant concentration in the prey are constant.

Dynamic ecological population models can offer insight on the variability of these biokinetic parameters and their influences on the trophic transfer of toxicants. Huang et al. (2014) developed a toxicant-mediated predator–prey model that incorporates a variable prey quantity. This model tracks the prey and predator population densities, as well as the toxicant body burdens in each population. The biokinetic model (1) corresponds with the predator body burden equation from Huang et al. (2014):

$$\underbrace{\frac{dv}{dt}}_{\text{Change in toxicant conc. of predator over time}} = \underbrace{a_2 T}_{\text{uptake from water}} + \underbrace{\xi f(x) u}_{\text{uptake from consuming prey}} - \underbrace{\sigma_2 v}_{\text{loss due to efflux}} - \underbrace{e(v) f(x) v}_{\text{loss due to growth}} \quad (2)$$

where $e(v)$ is the toxicant dependent biomass conversion efficiency. The original constant ingestion rate f is replaced with function $f(x)$ and depends on prey quantity; the constant predator growth rate g is replaced with the expression $e(v)f(x)$ and depends on the prey quantity, as well as, the predator's toxicant concentration. Huang et al. (2014) parameterize their model with the toxicant mercury (Hg), a toxic contaminant that can bioaccumulate in aquatic food chains as methylmercury (MeHg) posing risk to ecosystems and humans (Mergler et al., 2007). Their toxicant-mediated predator–prey model helped shed light on the different complicated ways varying toxicant concentrations affects organisms at different trophic levels.

While this model incorporates variable food quantity, it does not consider food quality. Elemental imbalances, such as phosphorus:carbon (P:C) ratios, between trophic levels affect life-history traits such as growth and reproduction. Toxic compounds can have similar impacts on these traits. There is increasing evidence that considering resource stoichiometry and nutrient availability will improve risk assessment protocols in ecotoxicology (Ieromina et al., 2014; Sarwar et al., 2010; Lessard and Frost, 2012; Alexander et al., 2013). The interactive effects of nutrient availability and aqueous Hg concentration may play a significant role in the bioaccumulation of MeHg. Karimi et al. (2007) show stoichiometric constraints, such as food quality, can affect the accumulation of MeHg in *Daphnia*. They show empirical evidence of Somatic Growth Dilution (SGD) as *Daphnia* experience a greater than proportional gain in biomass relative to MeHg under high phosphorus concentrations (Fig. 1). They used MeHg radio-tracer to measure juvenile *Daphnia pulex* MeHg concentrations, growth rate, and ingestion rate when fed on *A. falcatus* algae of low and high quality (vary algal P:C ratio). Estimated *Daphnia* steady-state MeHg concentrations using the biokinetic model (System (1)) showed that *Daphnia* grown on high quality food had 3.5 times higher growth rates, slightly lower ingestion rates, and MeHg concentrations at steady-state a third lower than *Daphnia* grown on low quality food.

Given this empirical evidence, the interactive effects of resource limitation and contaminant stress on organisms and ecosystems needs to be considered in toxicological risk assessment applications. Models have proven to be useful tools in ecotoxicological predictions, however current models do not consider dynamical interactive effects of contaminant stressors and stoichiometric constraints, such as nutrient/light availability and food quality.

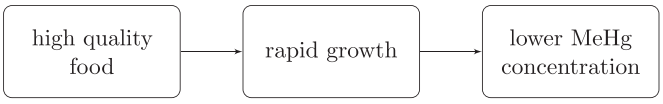

Fig. 1. Simple depiction of Somatic Growth Dilution (SGD), where an organism experiences a greater than proportional gain in biomass relative to toxicant under high food quality conditions.

In order to incorporate and balance multiple essential elements and contaminants, the mathematical models and the empirical experiments will be structured under the framework of the theory of Ecological Stoichiometry (Sterner and Elser, 2002). This theory considers the balance of multiple chemical elements and how the relative abundance of essential elements, such as carbon (C), nitrogen (N), and phosphorus (P), in organisms affects ecological dynamics. Ecologists have made important progress collecting large amounts of data from both lab experiments and field sites to support Ecological Stoichiometry (Andersen, 1997; Sterner and Elser, 2002; Urabe and Sterner, 1996; Elser et al., 1996; Elser and Urabe, 1999; Elser et al., 2000, 2001; Urabe et al., 2002; McCauley et al., 2008; Hessen et al., 2013). Since the development of the theory of ecological stoichiometry, a wide variety of stoichiometric food web models have been proposed and analyzed (Andersen, 1997; Loladze et al., 2000; Grover, 2004; Hall, 2004; Wang et al., 2008a; Hall, 2009; Wang et al., 2012; Peace et al., 2013, 2014). Stoichiometric models incorporate the effects of both food quantity and food quality into a single framework that produces rich dynamics. Stoichiometric models allow one to investigate the effects of nutrient stressors on population dynamics and track the trophic transfer of energy and nutrients (Peace, 2015). Empirical efforts and models developed under the theory of Ecological Stoichiometry have advanced our understanding of ecological interactions (Andersen et al., 2004; Hessen et al., 2013).

Two existing ecotoxicology models do consider a contaminant stressor along with a single stoichiometric constraint: (1) Bontje et al. (2009) developed a model that considers both nutrient stress and toxicant stress parameterized for a *N*-limited algal population and (2) Ankley et al. (1995) developed a model that considers both light availabilities and contaminant concentrations to looks at the effects of varying light intensities on a photo-activated contaminant stressor on aquatic organisms. However, unlike Ecological Stoichiometric models, these models do not allow for multiple dynamic stoichiometric constraints where the element limiting growth can change with environmental nutrient and light availabilities.

Ecological Stoichiometry has proven successful in aquatic ecological applications and has the potential to improve our understanding of the effects chemical contaminants have on organisms and ecosystems (Hansen et al., 2008). It offers a conceptual framework to investigate the impact of elemental imbalances on the response of organisms to contaminants while simultaneously considering the effects of contaminants on ecosystem processes (Danger and Maunoury-Danger, 2013).

Here, we extend System (3) under the framework of Ecological Stoichiometry (Sterner and Elser, 2002) to develop a toxicant-mediated predator–prey model that incorporates a variable food quantity as well as quality. Loladze et al. (2000) formulated a stoichiometric predator–prey Lotka–Volterra type model (LKE model) of the first two trophic levels of an aquatic food chain incorporating the fact that both the predator and prey are chemically heterogeneous organisms composed of two essential elements, carbon (C) and phosphorus (P). The model allows the phosphorus to carbon ratio (P:C) of the prey to vary above a minimum value, which brings food quality into the model. The LKE model is described in detail in Appendix A and is used as guide as we expand System (3) under the Ecological Stoichiometric framework. These modeling efforts help shed light on nutrient and chemical contaminant cycling and ultimately can improve toxicological risk assessment protocols.

2. Model formulation

We start with the toxicant-mediated predator–prey model developed by Huang et al. (2014):

$$\underbrace{\frac{dx}{dt}}_{\text{Change in prey density over time}} = \underbrace{b(u,x)x}_{\text{gain from growth}} - \underbrace{d_1(u)x}_{\text{loss from death}} - \underbrace{f(x)y}_{\text{loss from predation}} \tag{3a}$$

$$\underbrace{\frac{dy}{dt}}_{\text{Change in predator density over time}} = \underbrace{e(v)f(x)y}_{\text{gain from growth}} - \underbrace{d_2(v)y}_{\text{loss from death}} \tag{3b}$$

$$\underbrace{\frac{du}{dt}}_{\text{Change in toxicant in prey over time}} = \underbrace{a_1T}_{\text{uptake from water}} - \underbrace{\sigma_1 u}_{\text{efflux}} - \underbrace{b(u,x)u}_{\text{loss due to growth}} \tag{3c}$$

$$\underbrace{\frac{dv}{dt}}_{\text{Change in toxicant in predator over time}} = \underbrace{a_2T}_{\text{uptake from water}} - \underbrace{\sigma_2 v}_{\text{efflux}} + \underbrace{\xi f(x)u}_{\text{uptake from prey}} - \underbrace{e(v)f(x)v}_{\text{loss due to growth}} \tag{3d}$$

where x and y are the prey and predator population densities (mg C/L) respectively and u and v give toxicant body burden, or the concentrations of the toxicant in the prey and predatory, respectively. Function $b(u,x)$ is the toxicant dependent prey growth rate, $d_1(u)$ and $d_2(v)$ are toxicant dependent death rates for the prey and predator, respectively, $f(x)$ is the predator ingestion rate, $e(v)$ is the toxicant dependent biomass conversion efficiency, a_1, a_2 are toxicant uptake rates and σ_1, σ_2 are toxicant efflux rates for the prey and predator, respectively, and ξ is the predator toxicant assimilation efficiency.

We extend System (3) under the framework of Ecological Stoichiometry (Sterner and Elser, 2002) to develop a toxicant-mediated predator–prey model that incorporates a variable food quantity as well as quality. First, consider the prey growth rate presented in Huang et al. (2014),

$$b(u,x) = \frac{\alpha_1 \max\{0, 1-\alpha_2 u\}}{1+\alpha_3 x}$$

where $0 \le \max\{0, 1-\alpha_2 u\} \le 1$ comes from a linear dose response for the gain rate. Parameter α_1 is the maximum prey growth rate, α_2 is the effect of the toxicant on the prey growth rate, and α_3 accounts for the effect of crowding on the prey. Logistic growth is commonly used in the Ecological Stoichiometry framework, as the carrying capacity is easily modified to depend on carbon (light) and P availability. Here we represent growth with a logistic growth expression where the linear dose response gain rate is incorporated into the maximum growth rate parameter:

$$b(u,x,y) = \alpha_1 \max\{0, 1-\alpha_2 u\}\left(1 - \frac{x}{\min\left\{K, \dfrac{P-\theta y}{q}\right\}}\right) \tag{4}$$

Here α_1 is the maximum intrinsic growth rate of the prey and the above logistic growth expression includes any natural morality of the prey, K is the prey carrying capacity in terms of carbon or light availability, P is the total about of phosphorus in the system, θ is the constant predator P:C ratio, q is the minimum P:C ratio of the prey, and Q is the variable prey P:C ratio:

$$Q = \frac{P-\theta y}{x}. \tag{5}$$

The above equation is based on the assumption that all available nutrients are either in the prey or the predator. The model does not allow for free nutrients to be in the environment. This assumption is based on the fact that algae take up nutrients very quickly. This is also assumed in Loladze et al. (2000). Relaxation of this assumption has been investigated in stoichiometric models that track free nutrients in the environment (Wang et al., 2008a; Peace et al., 2014). A minimum function is used to describe the prey carrying capacity, $\min\{K, (P-\theta y)/q\}$. The first input, K, is the carrying capacity determined by light availability. The second input, $(P-\theta y)/q$ is the carrying capacity determined by phosphorus availability.

Now, consider the predator's conversion efficiency presented in Huang et al. (2014),

$$e(v) = \beta_1 \max\{0, 1-\beta_2 v\}$$

where $0 < \beta_1 < 1$ is the growth efficiency, and $\max\{0, 1-\beta_2 v\}$ represents a linear dose response for the growth efficiency where β_2 is the effect of the toxicant on predator growth. Under the stoichiometric framework, predator growth efficiency depends on the prey's variable P:C ratio Q and the predator's constant P:C ratio θ. A portion of the ingested carbon is used for the predator's metabolic costs, such as respiration. Let β_1 be the predator's maximal production efficiency in terms of carbon. Then $\frac{Q}{\beta_1}$ is the P:C ratio of the post-ingested prey representing the amount of P and C available for predator growth. When $\frac{Q}{\beta_1} > \theta$, the growth of the predator is limited by carbon and the maximum conversion efficiency is β_1. However when $\frac{Q}{\beta_1} < \theta$, the growth of the predator is limited by phosphorus and the maximum conversion efficiency is $\frac{Q}{\theta}$. The predator's conversion efficiency takes the following form:

$$e(v,x,y) = \min\left\{\beta_1, \frac{Q}{\theta}\right\}\max\{0, 1-\beta_2 v\}. \tag{6}$$

Note that β_1 corresponds with the parameter e in the LKE model as the predator's conversion efficiency in terms of carbon. A minimum function is used to describe the consumer growth rate, $\min\left\{\beta_1, \frac{Q}{\theta}\right\}$. The first input, β_1, is used when consumer growth is limited by carbon. The second input, $\frac{Q}{\theta}$ is used when consumer growth is limited by phosphorus.

Incorporating the stoichiometric logistic growth expression for the prey (4) and conversion efficiency for the predator (6) yields the following toxicant-mediated model that incorporates a variable food quantity as well as quality:

$$\underbrace{\frac{dx}{dt}}_{\text{Change in prey density over time}} = \underbrace{\alpha_1 \max\{0, 1-\alpha_2 u\}\left(1 - \frac{x}{\min\left\{K, \frac{P-\theta y}{q}\right\}}\right)x}_{\text{gain from growth}} - \underbrace{f(x)y}_{\text{loss from predation}} \tag{7a}$$

$$\underbrace{\frac{dy}{dt}}_{\text{Change in predator density over time}} = \underbrace{\min\left\{\beta_1, \frac{Q}{\theta}\right\}\max\{0, 1-\beta_2 v\}f(x)y}_{\text{gain from growth}} - \underbrace{d_2(v)y}_{\text{loss from death}} \tag{7b}$$

$$\underbrace{\frac{du}{dt}}_{\substack{\text{Change in toxicant}\\ \text{of prey over time}}} = \underbrace{a_1 T}_{\substack{\text{uptake from}\\ \text{water}}} - \underbrace{\sigma_1 u}_{\substack{\text{loss due to}\\ \text{efflux}}} - \underbrace{\alpha_1 \max\{0,\, 1-\alpha_2 u\}\left(1 - \frac{x}{\min\left\{K, \frac{P-\theta y}{q}\right\}}\right)u}_{\substack{\text{loss due to}\\ \text{growth}}} \tag{7c}$$

$$\underbrace{\frac{dv}{dt}}_{\substack{\text{Change in toxicant}\\ \text{of predator over time}}} = \underbrace{a_2 T}_{\substack{\text{utake from}\\ \text{water}}} + \underbrace{\xi f(x) u}_{\substack{\text{uptake from}\\ \text{prey}}} - \underbrace{\sigma_2 v}_{\substack{\text{loss due to}\\ \text{efflux}}} - \underbrace{\min\left\{\beta_1, \frac{Q}{\theta}\right\}\max\{0,\, 1-\beta_2 v\} f(x) v}_{\substack{\text{loss due to}\\ \text{growth}}}. \tag{7d}$$

The biokinetic model (1) corresponds with $\frac{dv}{dt}$ from Eq. (7d). The original constant ingestion rate f is replaced with function $f(x)$ and depends on prey quantity; the constant predator growth rate g is replaced with the expression $e(v, x, y)f(x)$ and depends on the prey quantity and quality, as well as, the predator's toxicant concentration.

3. Model parameterization

We apply the stoichiometric toxicant-mediated predator–prey model (7) to a system of algae (prey) and *Daphnia* (predator), in order to investigate the effects of co-occurring phosphorus and Hg availabilities on population dynamics and Hg bioaccumulation. Details on the parameterization are in Appendix B. All parameter values are listed in Table 1.

4. Model analysis

We assume the dynamics of the body burden equations (7 c,d) operate on a faster time scale than the dynamics of population growth (7 a,b). The uptake and efflux of the toxicant may balance out and drive the body burden equations to approach a quasi-steady-state. For the model analysis we make this quasi-steady-state assumption to reduce the system down to two equations. Define the small parameter $\epsilon = \alpha_1\sigma_1$. Note that using the parameters in Table 1 for algae and *Daphnia* $\epsilon = 0.0576$. This small parameter is introduced in the following nondimensionalization. We then analyze the reduced nondimensional system. For mathematical convenience, we assume $I=1$ for the following analysis. The parameterization of this simplifying assumption on the mortality function is discussed in Appendix B.

4.1. Nondimensionalization and quasi-steady-state approximation

Here we rescale the Model (7) with the following nondimensional parameters:

$$\begin{aligned}
&\tilde{u} = \alpha_2 u, \quad \widetilde{m_2} = \frac{m_2}{\alpha_1}, \quad \widetilde{\beta_1} = \frac{c\beta_1}{\alpha_1}, \quad \widetilde{\beta_2} = \frac{\xi c \sigma_1 \beta_2}{\alpha_2},\\
&\gamma = \frac{a_2\beta_2}{\alpha_2 a_1}, \quad \tilde{v} = \beta_2 v, \quad \epsilon = \alpha_1\sigma_1, \quad \tilde{t} = \alpha_1 t,\\
&\widetilde{\sigma_2} = \sigma_2\sigma_1, \quad \sigma_1 = \sigma_1, \quad \tilde{T} = \alpha_2 a_1 \sigma_1 T, \quad \tilde{y} = \frac{c}{\alpha_1} y,\\
&\widetilde{h_1} = \frac{h_1}{\alpha_1\alpha_2}, \quad \widetilde{h_2} = \frac{h_2}{\beta_2\alpha_1}, \quad \tilde{\theta} = \frac{\alpha_1\theta}{c}, \quad \widetilde{Q} = \frac{P - \tilde{\theta}\tilde{y}}{x}.
\end{aligned} \tag{8}$$

Dropping the tildes for more convenient notation, Model (7) can then be written as the following nondimensional system:

$$\frac{dx}{dt} = \max\{0,\, 1-u\}\left(1 - \frac{x}{\min\left\{K, \frac{P-\theta y}{q}\right\}}\right)x - \frac{xy}{a+x} \tag{9a}$$

$$\frac{dy}{dt} = \min\left\{\beta_1, \frac{Q}{\theta}\right\}\max\{0,\, 1-v\}\frac{xy}{a+x} - (h_2 v + m_2)y \tag{9b}$$

Table 1
Model parameters.

Parameter	Description	Value	Source
α_1	Algae maximal growth rate	1.2/day	Andersen (1997)
α_2	Toxicant effect on algal reproduction	0.0051 mg C/μg T	Estimated from data compiled in Vocke (1978)[a]
K	Algae C carrying capacity	0–3 mg C/L	Andersen (1997)
β_1	*Daphnia* C growth efficiency	0.8 (unitless)	Andersen (1997)
β_2	Toxicant effect on *Daphnia* reproduction	10.13 mg C/μg T	Fit to data from Biesinger et al. (1982)[b]
θ	*Daphnia* constant P:C	0.03 mg P/mg C	Andersen (1997)
q	Algae minimal P:C	0.0038 mg P/mg C	Andersen (1997)
h_2	Toxicant coefficient for *Daphnia* mortality	0.347 mg C/μg T/day	Fit to data from Biesinger et al. (1982)[c]
I	Toxicant exponent for *Daphnia* mortality	1.685 (unitless)	Fit to data from Biesinger et al. (1982)[c]
m_2	*Daphnia* natural loss rate	0.25/day	Andersen (1997)
c	*Daphnia* max ingestion rate	0.81/day	Andersen (1997)
a	*Daphnia* ingestion half saturation constant	0.25 mg C/L	Andersen (1997)
a_1	Algae uptake coefficient	0.012 L/mg C/day	Hill and Larsen (2005)
a_2	*Daphnia* uptake coefficient	0.011 L/mg C/day	Tsui and Wang (2004)
σ_1	Algae toxicant efflux rate	0.048/day	Hill and Larsen (2005)
σ_2	*Daphnia* toxicant efflux rate	0.04/day	Tsui and Wang (2004), Karimi et al. (2007)
ξ	*Daphnia* toxicant assimilation efficiency	0.97 (unitless)	Tsui and Wang (2004), Karimi et al. (2007)
T	Total toxicant	μg T/L	
P	Total phosphorus	mg 0.01–0.08 mg P/L	

[a] Parameter estimation discussed in Section B.2.
[b] Data fitting discussed in Section B.3.2.
[c] Data fitting discussed in Section B.3.1.

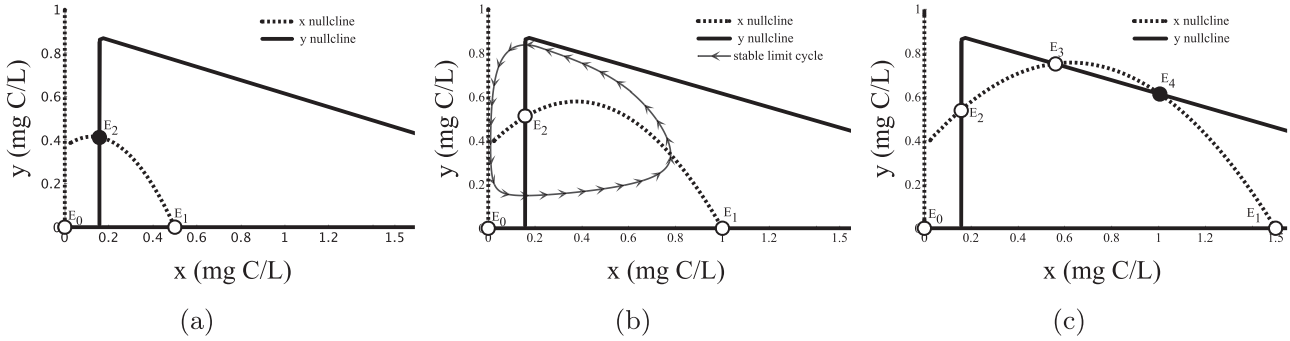

Fig. 2. Predator–prey phase portraits for varying light levels: (a) low light $K=0.5$ mg C/L, (b) high light $K=1$ mg C/L, (c) very high light $K=1.5$ mg C/L. The x-nullclines are dashed curves and the y-nullclines are solid curves. Open circles depict unstable equilibria and closed circles depict locally stable equilibria. Points E_0 and E_1 are boundary equilibria. Points E_2, E_3, and E_4 are interior equilibria. The grey arrowed-curve in figure (b) shows a stable limit cycle. Parameter values listed in Table 1 with $P=0.03$ mg P/L and $T=0.025$ μg MeHg/L. Population dynamics are similar to those obtained in Loladze et al. (2000).

$$\epsilon\frac{du}{dt} = T - \sigma_2^2 u - \epsilon\max\{0, 1-u\}\left(1 - \frac{x}{\min\left\{K, \frac{P-\theta y}{q}\right\}}\right)u \tag{9c}$$

$$\epsilon\frac{dv}{dt} = \gamma T - \sigma_2 v + \left[\beta_2 u - \epsilon\min\left\{\beta_1, \frac{Q}{\theta}\right\}\max\{0, 1-v\}v\right]\frac{x}{a+x} \tag{9d}$$

Applying the quasi-steady-state assumption and letting $\epsilon \to 0$ yields

$$u = \frac{T}{\sigma_1^2}, \quad v = \frac{T}{\sigma_2}\left(\gamma + \frac{\beta_2}{\sigma_1^2}\frac{x}{a+x}\right). \tag{10}$$

Substituting (10) into the x and y equations of System (9) produces the following quasi-steady-state nondimensional system:

$$\frac{dx}{dt} = \max\left\{0, 1-\frac{T}{\sigma_1^2}\right\}\left(1 - \frac{x}{\min\left\{K, \frac{P-\theta y}{q}\right\}}\right)x - \frac{xy}{a+x} \tag{11a}$$

$$\frac{dy}{dt} = \min\left\{\beta_1, \frac{Q}{\theta}\right\}\max\left\{0, 1-\frac{T}{\sigma_2}\left(\gamma + \frac{\beta_2}{\sigma_1^2}\frac{x}{a+x}\right)\right\}\frac{xy}{a+x} - \left(\frac{h_2 T}{\sigma_2}\left(\gamma + \frac{\beta_2}{\sigma_1^2}\frac{x}{a+x}\right) + m_2\right)y \tag{11b}$$

Note that if $T > \sigma_1^2$ then the toxicant levels are too high for the prey to reproduce and grow and $(x, y) \to (0, 0)$. For the following analysis we assume that $T < \sigma_1^2$ and let $\mathbf{k} = \min\left\{K, \frac{P}{q}\right\}$.

4.2. Positive invariance

Theorem 4.1. *Solutions to System (11) with initial conditions in the set*

$$\Omega = \left\{(x, y): 0 \le x \le \mathbf{k} = \min\left\{K, \frac{P}{q}\right\}, \quad 0 \le y,\ qx + \theta y < P\right\} \tag{12}$$

will remain there for all forward time.

The proof can be found in Appendix D.

4.3. Asymptotic dynamics

To investigate the equilibria we first rewrite System (11) in the following form:

$$\frac{dx}{dt} = xF(x, y) \tag{13a}$$

$$\frac{dy}{dt} = yG(x, y) \tag{13b}$$

where

$$F(x, y) = \max\left\{0, 1-\frac{T}{\sigma_1^2}\right\}\left(1 - \frac{x}{\min\left\{K, \frac{P-\theta y}{q}\right\}}\right) - \frac{y}{a+x} \tag{14a}$$

$$G(x, y) = \min\left\{\beta_1, \frac{Q}{\theta}\right\}\max\left\{0, 1-\frac{T}{\sigma_2}\left(\gamma + \frac{\beta_2}{\sigma_1^2}\frac{x}{a+x}\right)\right\}\frac{x}{a+x} - \left(\frac{h_2 T}{\sigma_2}\left(\gamma + \frac{\beta_2}{\sigma_1^2}\frac{x}{a+x}\right) + m_2\right) \tag{14b}$$

The Jacobian takes the following form:

$$J = \begin{vmatrix} F(x, y) + xF_x(x, y) & xF_y(x, y) \\ yG_x(x, y) & G(x, y) + yG_y(x, y) \end{vmatrix}.$$

There are two equilibria on the boundary, $E_0 = (0, 0)$ and $E_1 = (\mathbf{k}, 0)$. The following theorem shows local stability of these boundary equilibria.

Theorem 4.2. *$E_0 = (0, 0)$ is saddle point. The stability of $E_1 = (\mathbf{k}, 0)$ depends on the sign of $G(\mathbf{k}, 0)$. E_1 is locally asymptotically stable if $G(\mathbf{k}, 0) < 0$ and E_1 is saddle point if $G(\mathbf{k}, 0) > 0$.*

The proof can be found in Appendix E.

Fig. 2 illustrates phase portraits with the prey x-nullclines and the predator y-nullclines for varying levels of light. Equilibria are located at the intersection of these nullclines. In addition to the two boundary equilibria E_0 and E_1, numerical observations show the existence of three interior equilibria E_2, E_3, and E_4. As light levels vary, the shape of the x-nullcline changes which affects the number and the nature of the interior equilibria. For low light (Fig. 2a) there is one interior equilibria, E_2. Numerical observations show that this is locally stable. For high light (Fig. 2b) this interior equilibria E_3 becomes unstable and a stable limit cycles emerges. Under very high light (Fig. 2c) there are three interior equilibria E_2, E_3, and E_4. Here the limit cycles have collapsed and E_4 is locally stable.

5. Numerical analysis

Loladze et al. (2000) investigate the effects of light enrichment on the basic stoichiometric predator–prey model (System (A1)). Peace et al. (2013) investigate the effects of nutrient enrichment on an expanded stoichiometric predator–prey model. It is observed that increasing light levels K causes the prey food quality Q to decrease, whereas increasing the nutrient levels P causes the prey food quality to increase. Here we numerically explore how stoichiometric constraints affect the populations densities and the trophic transfer of the toxicant. We vary the light level K, in order to manipulate the prey food quality. Additionally, we investigate the effects of increasing toxicant concentrations T on the population dynamics. Simulations from numerical experiments are presented in Section 5.1 and bifurcation analyses are presented in Section 5.2.

5.1. Numerical simulations

These simulations use the parameters listed in Table 1 with $P=0.03$ mg P/L for varying light intensities K (Fig. 3) and varying toxicant concentrations T (Fig. 4).

Fig. 3 shows the population densities, food quality, body burden, and phase portraits predicted by model (7) for three different light

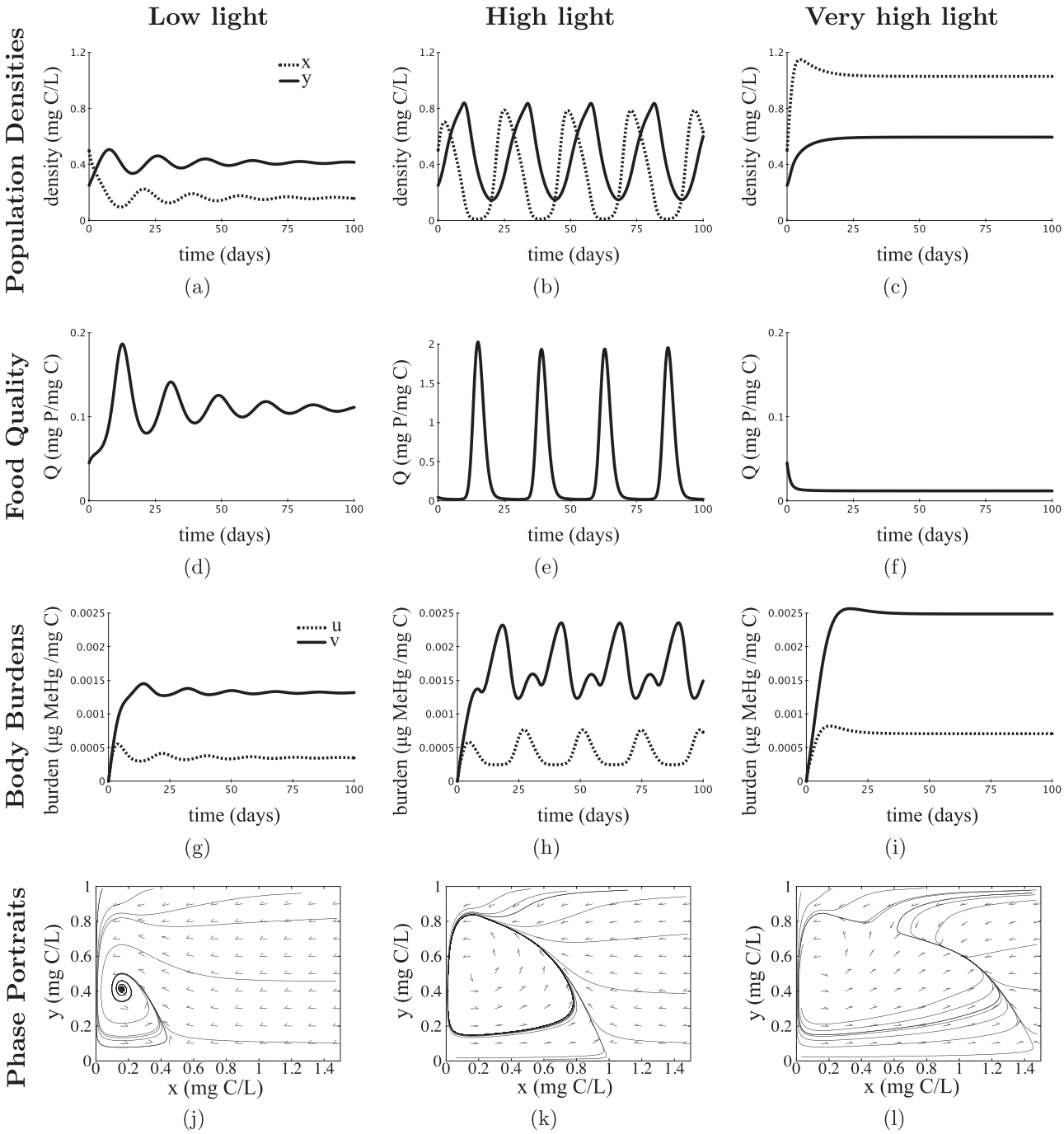

Fig. 3. Numerical simulations for (a)–(c) population densities x (dashed), y (solid) mg C/L, (d)–(f) algal quota Q mg P/mg C, (g)–(i) body burdens u (dashed), v (solid) μg MeHg/mg C, and (j)–(l) phase portraits for three different light intensities: low light $K=0.5$ mg C/L (column one), high light $K=1$ mg C/L (column two), and very high light $K=1.5$ mg C/L (column three). Parameter values listed in Table 1 with $P=0.03$ mg P/L and $T=0.025$ μg MeHg/L. Data obtained using MATLAB and XPP. Population dynamics are similar to those obtained in Loladze et al. (2000).

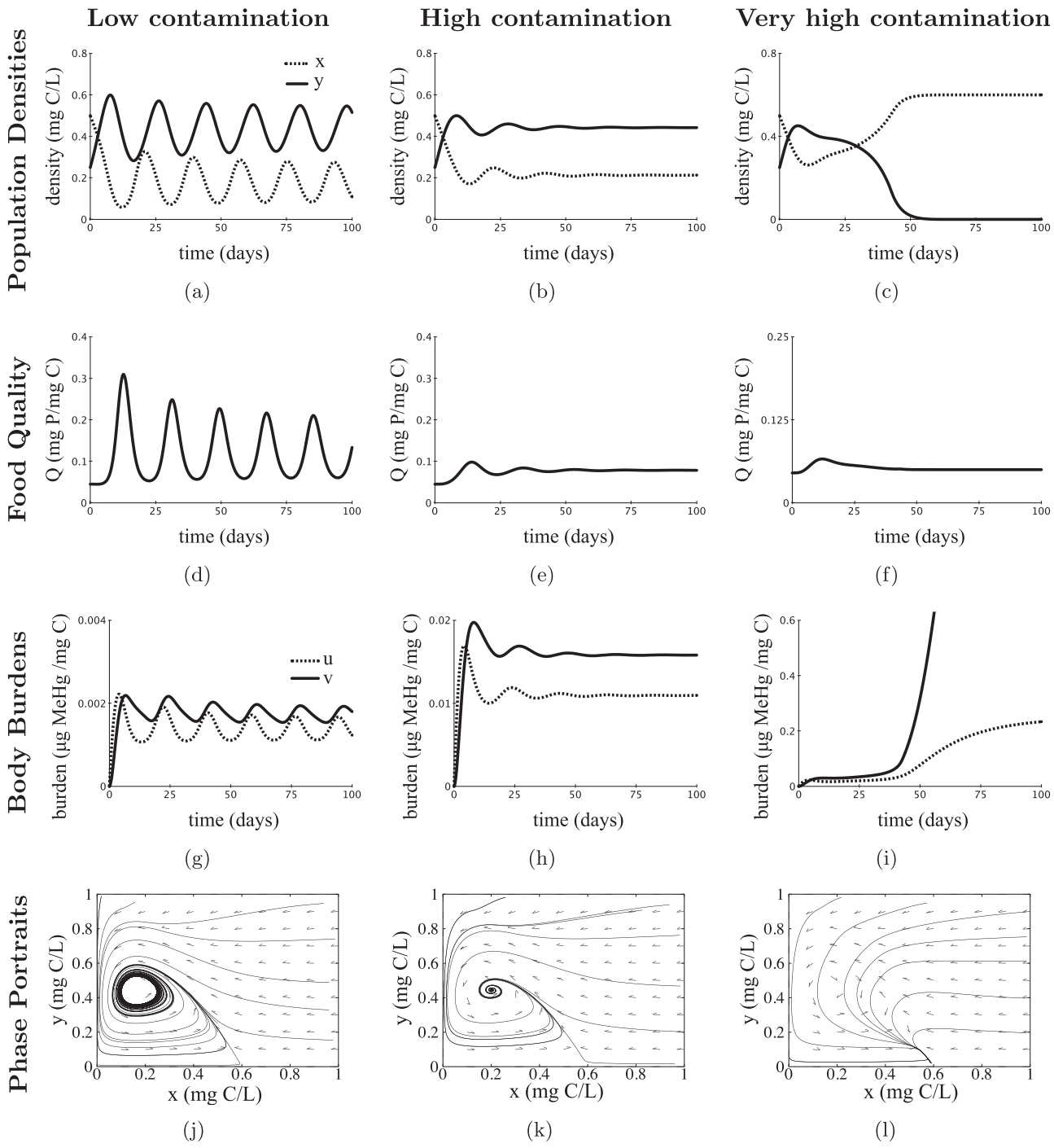

Fig. 4. Numerical simulations for (a)–(c) population densities x (dashed), y (solid) mg C/L, (d)–(f) algal quota Q mg P/mg C, and (g)–(i) body burdens u (dashed), v (solid) μg MeHg/mg C, and (j)–(l) phase portraits for three different MeHg toxicant levels: low contamination $T = 0.1$ μg MeHg/L (column one), medium contamination $T=0.5$ μg MeHg/L (column two), and high contamination $T = 1$ μg MeHg/L (column three). Parameter values listed in Table 1 with $P=0.03$ mg P/L and $K=0.6$ mg C/L. Data obtained using MATLAB and XPP.

levels $K=0.5$, 1, 1.5 mg C/L and a fixed toxicant level. The food quality Q predictions (Fig. 3d–f) follow from Eq. (5). Under low light, the system exhibits a stable steady state where the population densities x, y are low (Fig. 3a), food quality Q is high (Fig. 3d), and predator body burden u is low (Fig. 3g). Here y is low due to low food quantity. Increasing the light level to high light causes a Hopf bifurcation to occur as the steady state looses stability and limit cycles emerge (Fig. 3b, e, and h). The limit cycles collapse as the light level continues to increase. Under very high light, the system exhibits another stable steady state where the population density x is high but y is low (Fig. 3c), food quality Q is low (Fig. 3f), and predator body burden v is high (Fig. 3g). Here y is low due to low food quality rather than quantity. The low food quality (Fig. 3f) has significant influences on the predator population; reducing the density (Fig. 3c) and increasing the body burden (Fig. 3i). The Somatic Growth Dilution (SGD) effect is seen when comparing the food quality and body burden under low light (Fig. 3d and g) versus very high light (Fig. 3f and i).

Asymptotic dynamics can been seen in the phase portraits (Fig. 3j, k, and l). Under low light levels, the interior equilibria E_2 is stable (Fig. 3j). The existence of a stable limit cycle is observed under high light (Fig. 3k). Under very high light levels, the interior equilibria E_4 is stable (Fig. 3l).

Fig. 4 shows the population densities, food quality, body burden, and phase portraits predicted by model (7) for three different toxicant levels $T=0.5, 0.75, 1$ μg MeHg/L and a fixed light level. The food quality Q predictions (Fig. 4d–f) follow from Eq. (5). Under low toxicant contamination, the system exhibits limit cycles for this fixed light level $K=0.6$ mg C/L (Fig. 4a, d, and g). Increasing the toxicant contamination collapses the limit cycles as the system passes the Hopf bifurcation and exhibits a stable steady state (Fig. 4b, e, and h). Increasing the toxicant contamination further leads the predator population to extinction (Fig. 4c). Here the prey actually benefits from high contamination levels. According to the parameter values obtained, the algae are much less sensitive to MeHg contamination than *Daphnia* and the extinction of the predator relieves predation pressure off the prey (Fig. 4c). The increased population density of the prey x, under high contamination, reduces the prey food quality Q (Fig. 4f). The body burdens u, v increase as the toxicant levels increase. Under high contamination the predator body burden v increases very rapidly as the predator goes towards extinction $y \to 0$ (Fig. 4i). Note the difference in the scale on the vertical axes of Fig. 4g, h, and i.

Asymptotic dynamics can been seen in the phase portraits (Fig. 4j, k, and l). Under low toxicant contamination, there exists of a stable limit cycle (Fig. 4j). The interior equilibria E_4 is stable under high contamination (Fig. 3k). Under very high contamination, there are no stable interior equilibria or limit cycles and boundary equilibria E_1 is stable. Here the very high toxicant levels drives the predator to extinction.

5.2. Bifurcation analysis

Bifurcation diagrams for the predator population density y, the total amount of toxicant in the predator population V, and the predator body burden v are shown in Figs. 5 and 6.

Fig. 5 uses the light level K as the bifurcation parameter. These bifurcations are similar to those obtained in the LKE model (Loladze et al., 2000) and globally investigated by Van Voorn et al. (2010), Li et al. (2011), and Xie et al. (2016). When light levels are very low there is not enough energy in the system to support the predator population. As K increases, a stable steady state emerges. The predator population starts off at low density (Fig. 5a) with low body burden (Fig. 5c). As K continues to increase, the predator density increases until the stable steady state looses it's stability and limit cycles emerge at a Hopf bifurcation. This is the well known "paradox of enrichment" (Rosenzweig, 1971; Diehl, 2007). Eventually, as K increases further, another bifurcation occur where the limit cycles collapse and a new interior stable state appears. For the LKE model, Van Voorn et al. (2010) found this bifurcation to be a homoclinic bifurcation coinciding with a tangent bifurcation where a saddle-node homoclinic connection is formed. After this bifurcation the predator density will begin to decrease as K increases to very high values. This decline in predator density caused by high light levels is a phenomenon called the "paradox of energy enrichment" (Loladze et al., 2000). At high light levels, the low density predator population has high body burden (Fig. 5c). The SGD effect is observed when comparing the body burden values on the left (low K) with the values on the right (high K) in Fig. 5c. Food quality Q is high for low light levels and is low for high light levels.

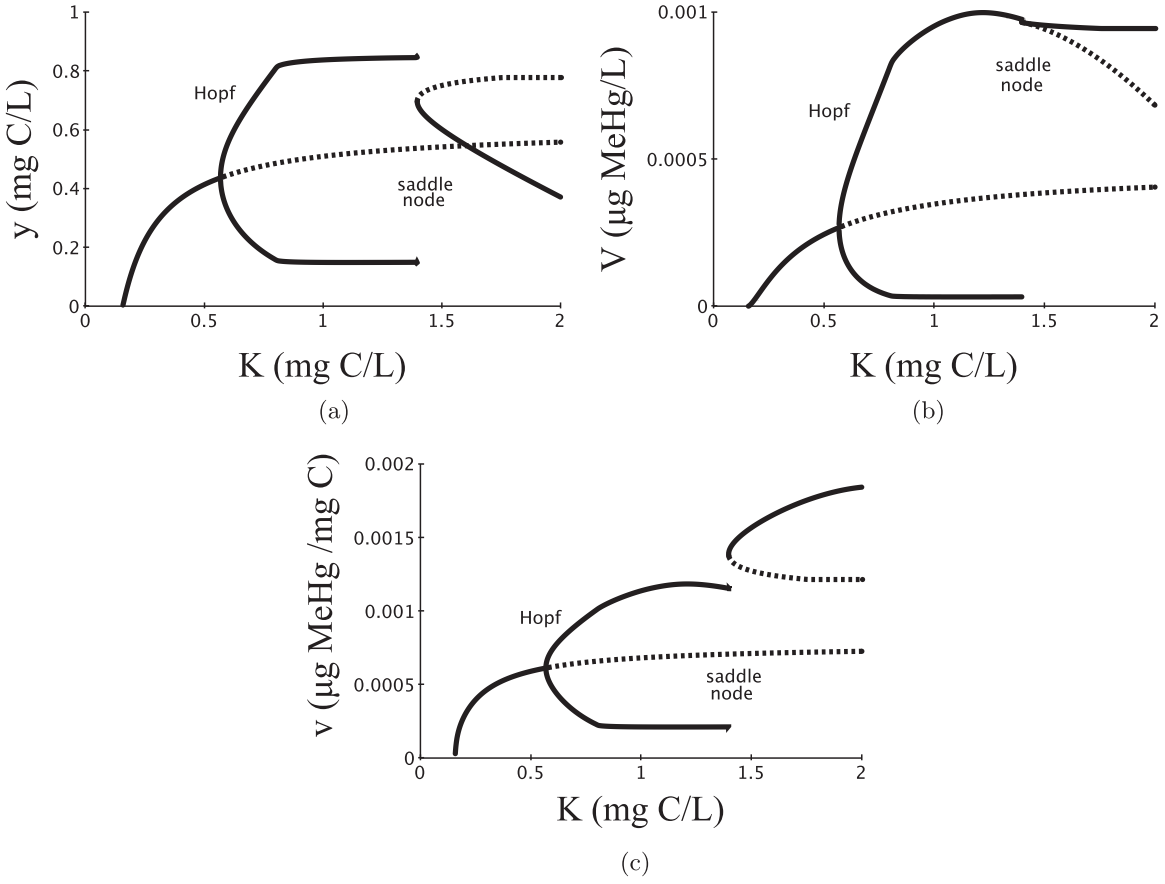

Fig. 5. Bifurcation diagrams for (a) y predator biomass, (b) V total toxicant in predator population, (c) v predator body burden using bifurcation parameter K mg C/L. Solid curves depict stable equilibria and limit cycles and dashed curves depict unstable equilibria. The solid curves in between the Hopf and saddle node bifurcations depict the maximum and minimum values of the stable limit cycle. Parameter values listed in Table 1 with $P=0.03$ mg P/L and $T=0.025$ μg MeHg/L. Data generated using XPP-AUTO. Population dynamics are similar to those obtained in Loladze et al. (2000) and globally investigated in Van Voorn et al. (2010), Li et al. (2011), and Xie et al. (2016).

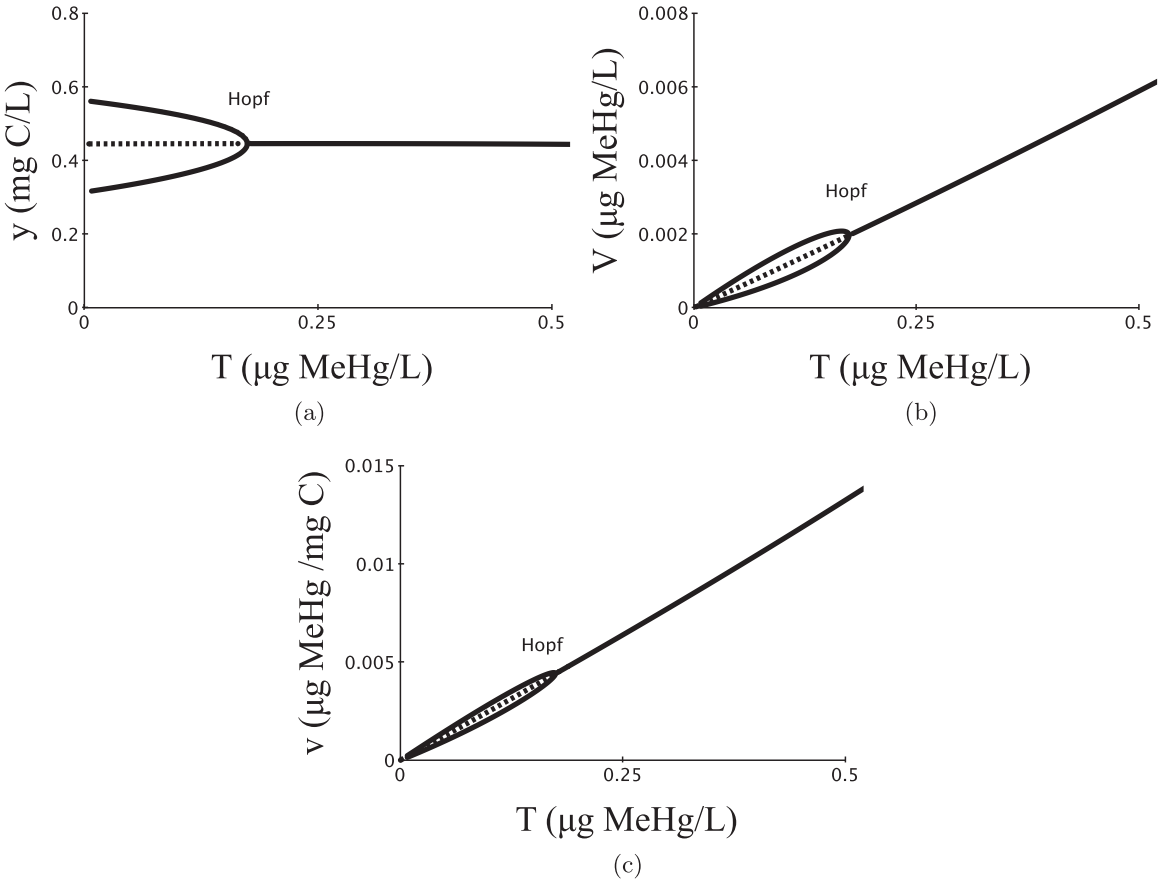

Fig. 6. Bifurcation diagrams for (a) y predator biomass, (b) V total toxicant in predator population, (c) v predator body burden using bifurcation parameter T μg MeHg/L. Solid curves depict stable equilibria and limit cycles and dashed curves depict unstable equilibria. The solid curves prior to the Hopf bifurcations depict the maximum and minimum values of the stable limit cycle. Parameter values listed in Table 1 with $P=0.03$ mg P/L and $K=0.6$ mg C/L. Data generated using XPP-AUTO.

Fig. 6 uses the toxicant contamination level T as the bifurcation parameter and a fixed light level $K=0.6$ mg C/L. Under this parameterization, the system exhibit limit cycles for low toxicant levels. As T increases, the limit cycles collapse at the Hopf bifurcation and a stable steady state emerges. The predator population experience a slight decrease as T, and therefore their body burden v increases. Eventually, for very high T levels not shown in the diagrams, the predator population will decline to extinction.

6. Discussion

The development of ecotoxicological models over the last couple decades have significantly contributed to interpreting how contaminants impact organisms and cycle through aquatic food webs (Hallam and De Luna, 1984; Ankley et al., 1995; Kooijman and Bedaux, 1996; Wang et al., 1996; Mackay et al., 1992; Pieters et al., 2006; Ashauer et al., 2007; Wang and Rainbow, 2008; Ashauer and Brown, 2008; Bontje et al., 2009; Huang et al., 2014). These modeling efforts take a variety of approaches to predict the effects of diverse chemical contaminants on organismal growth and survival. Many of these models assume the food quantity and quality are constant. (Huang et al., 2014 and Pieters et al., 2006 incorporate variable food quantities in their models but do not consider variable food quality.) However, there is increasing evidence that organisms experience interactive effects of contaminant stressors and food conditions, such as resource stoichiometry and nutrient availability (Danger and Maunoury-Danger, 2013).

We developed a model that expands conventional toxicological approaches that only consider constant food quantity and quality using the framework of Ecological Stoichiometry (Sterner and Elser, 2002). Model (7) incorporates the effects of concurrent nutrient and toxicant stressors on population dynamics and the trophic transfer of toxicants. While the model can be generalized to a variety of aquatic species and chemicals, we parameterized model (7) to an algae–*Daphnia* system that investigates levels of phosphorus, carbon (light), and MeHg.

In order to analytically analyze the model, we employed a quasi-steady-state assumption to reduce the model down to two dimensions. We assumed population metabolism occurs on a faster time scale than population growth dynamics. Analytical analysis of the reduced model (System (11)) shows the model is positive and bounded. We analytically investigated the existence and local stability of boundary equilibria. The existence and stability of interior equilibria and limit cycles were observed numerically.

Recent data show that the interactive effects of nutrient availability and aqueous Hg concentration may play a significant role in the bioaccumulation of MeHg. The model is used to explored the effects of varying light levels and toxicant concentrations on population dynamics and the flow of MeHg across the two trophic levels. The model captures the Somatic Growth Dilution (SGD) phenomenon, which has been observed empirically in *Daphnia* contaminated with MeHg, as they experience a greater than proportional gain in biomass relative to MeHg under high phosphorus concentrations (Karimi et al., 2007). SGD can be seen in the numerical simulations and bifurcation analysis (Section 5).

It is important to note that the nonstoichiometric toxicant-mediated predator prey model developed by Huang et al. (2014), model (3) and the stoichiometric model developed here, model (7) ignore the influences of the populations on the toxicant in the environment. Environmental toxicant concentration is treated as a parameter, T. These models assume the toxicant concentrations in

the environment are determined by external conditions and are not regulated by the population dynamics. This assumption is reasonable because the toxicant contained in the studied populations is a tiny portion of the environmental toxicant.

The model developed here integrates an a ecotoxicological model into the theory of Ecological Stoichiometry. Eqs. (4) and (6) are an initial attempt at coupling toxicant and nutrient stressors in the growth functions of the prey and predator. Here we assume that the organisms pay an energy or carbon cost when exposed to contaminants, that reduce the growth rates based on a linear dose response of growth to concentrations of the toxicant. The model allows us to mathematically explore toxicant-induced *carbon* costs. It is important to note that this initial model iteration assumes the toxicant-induced costs is paid in carbon.

Future model iterations should consider the impact of contaminants on organism elemental compositions. In addition to influencing life history traits specific contaminants can impact organism elemental composition (Danger and Maunoury-Danger, 2013). This phenomenon has recently been observed: Wang et al. (2008b) observed plants have lower nitrogen leaf concentrations when exposed to cadmium, and Xing et al. (2010) observed aquatic plants have lower nitrogen and phosphorus concentrations when exposed to iron or copper. Some chemical contaminants have the ability to alter an organism's physiology, such as their stoichiometric P:C ratio. Such impacts on the elemental composition will alter the elemental balances between the organisms and their consumed resources, resulting in stoichiometric constraints that will in turn influence population dynamics. More work is needed that focuses on how toxicants impact elements compositions. Future directions can mathematically and empirically explore toxicant-induced *nutrient* costs, in addition to the toxicant-induced *carbon* costs incorporated in the model presented here.

Acknowledgements

Part of this work was conducted while Angela Peace was Postdoctoral Fellow at the National Institute for Mathematical and Biological Synthesis, an Institute sponsored by the National Science Foundation through NSF Award #DBI-1300426, with additional support from The University of Tennessee, Knoxville. Hao Wang's research is partially supported by an NSERC Discovery grant.

Appendix A. LKE model with slight modification

Loladze et al. (2000) formulated a stoichiometric prey-predator Lotka-Volterra type model (LKE model) of the first two trophic levels of an aquatic food chain incorporating the fact that both preys and predators are chemically heterogeneous organisms composed of two essential elements, carbon (C) and phosphorus (P). The model allows the phosphorus to carbon ratio (P:C) of the prey to vary above a minimum value, which brings food quality into the model. Below is the LKE model presented by Loladze et al. (2000):

$$\frac{dx}{dt} = \alpha_1 x\left(1 - \frac{x}{\min\left\{K, \frac{P-\theta y}{q}\right\}}\right) - f(x)y \tag{A.1a}$$

$$\frac{dy}{dt} = e\min\left\{1, \frac{Q}{\theta}\right\} f(x)y - d_2 y \tag{A.1b}$$

where

$$Q = \frac{P-\theta y}{x},$$

and α_1 is the prey maximum growth rate, K is the prey carrying capacity in terms of carbon or light availability, P is the total about of phosphorus in the system, θ is the constant predator P:C ratio, Q is the variable prey P:C ratio, and q is the minimum P:C ratio of the prey.

Here, a minimum function is used to describe the prey carrying capacity, $\min\{K, (P-\theta y)/q\}$. The first input, K, is the carrying capacity determined by light availability. The second input, $(P-\theta y)/q$ is the carrying capacity determined by phosphorus availability. Another minimum function is used to describe the consumer growth rate, $\min\left\{1, \frac{Q}{\theta}\right\}$. The first input, 1, is used when consumer growth is limited by carbon. The second input, $\frac{Q}{\theta}$ is used when consumer growth is limited by phosphorus.

Here we make a small modification to the LKE model (A.1) to put e inside the minimum function in the expression for predator's growth. It is well known that not all carbon biomass of the prey ends up as carbon biomass of the predator. Some carbon is used for metabolic processes, such as respiration. This is represented by the predator's conversion efficiency $e < 1$. It is important to note that this constant is defined in terms of carbon. Therefore Q/e is the P:C of the post ingested prey available for predator's growth. Consider $g(x, y)$ the predator's growth rate. When $\frac{Q}{e} > \theta$, the growth of the predator is limited by carbon and satisfies $g(x, y) = f(x)e$. However when $\frac{Q}{e} < \theta$, the growth of the predator is limited by phosphorus and satisfies $g(x, y)\theta = f(x)Q$. Together, these two cases can be written as:

$$g(x, y) = \begin{Bmatrix} \frac{Q}{\theta} f(x) & \text{for } \frac{Q}{e} < \theta \\ ef(x) & \text{for } \frac{Q}{e} > \theta \end{Bmatrix} = \min\left\{e, \frac{Q}{\theta}\right\} f(x).$$

Appendix B. Parameterization

B.1. Nontoxicant-related parameters

Many of the nontoxicant-related parameters of algae and

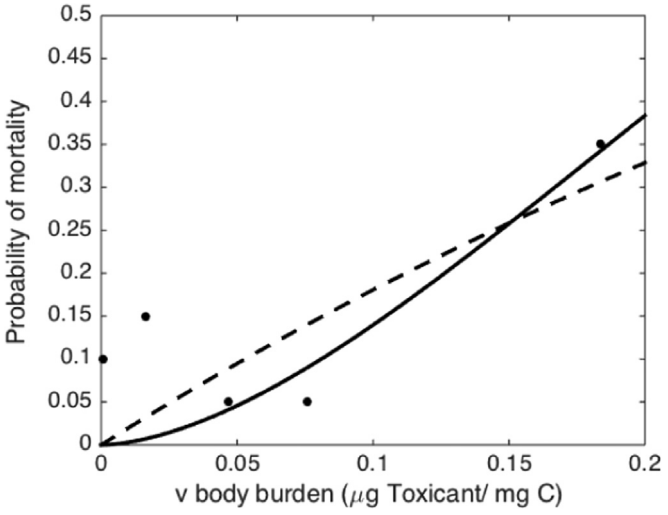

Fig. B1. Experimental data from Biesinger et al. (1982) of *Daphnia magna* exposed to MeHg for 21 days and the mortality function (B.3) with the obtained parameter values using MATLAB's LSQCURVEFIT to fit the data. The solid curve gives the empirical mortality function with parameters $h_2 = 0.347$ mg C/μg toxicant/day and $I = 1.685$. The dashed curve gives the simplified mortality function with parameters $h_2 = 0.0949$ mg C/μg toxicant/day and $I = 1$.

Daphnia population dynamics are biologically realistic values obtained from Andersen (1997), Urabe and Sterner (1996) and used in Loladze et al. (2000).

The predator's ingestion rate, $f(x)$ is a monotonic increasing and differentiable function, $f'(x) \geq 0$, $f(0) = 0$. $f(x)$ is saturating with $\lim_{x\to\infty} f(x) = c$. For the following analysis, we assume the ingestion rate is a Holling type II function of the following form,

$$f(x) = \frac{cx}{a + x}$$

where c is the maximal *Daphnia* ingestion rate and a is the half saturation constant.

B.2. Prey toxicant-related parameters

Hill and Larsen (2005) examined the uptake and elimination of Hg by microalgal biofilms. Their experiment involved observing microalgal biofilm Hg accumulation over a two day period where they measured the algae Hg uptake coefficient to be $a_1 = 0.0123$ L/mgC/day. They also observed the Hg loss rate by microalgal biofilms over a four day period and calculated the algal Hg efflux rate to be $\sigma_1 = 0.048$/day.

In order to estimate the effect of the toxicant on algae growth, consider the threshold body burden at which algae is no longer capable of growth. Following Huang et al. (2015), this threshold body burden can be described with the following equation,

$$\frac{1}{\alpha_2} = \frac{a_1}{\sigma_1} T_0 \tag{B.1}$$

where T_0 is the concentration of toxicant that inhibits algal growth 100%. Vocke (1978) compiled data of growth responses reported for freshwater algae exposed to Hg. Relevant data from Vocke (1978) on threshold Hg concentrations that resulted in 100% growth inhibition for various algal species is shown in Appendix C. The average Hg concentration threshold for complete inhibited growth across these species is $T_0 = 0.7843$ mg/L. Using this T_0 along with the above parameters for a_1 and σ_1 and Eq. (B.1), we estimate $\alpha_2 = 0.0051$ mg C/μg toxicant.

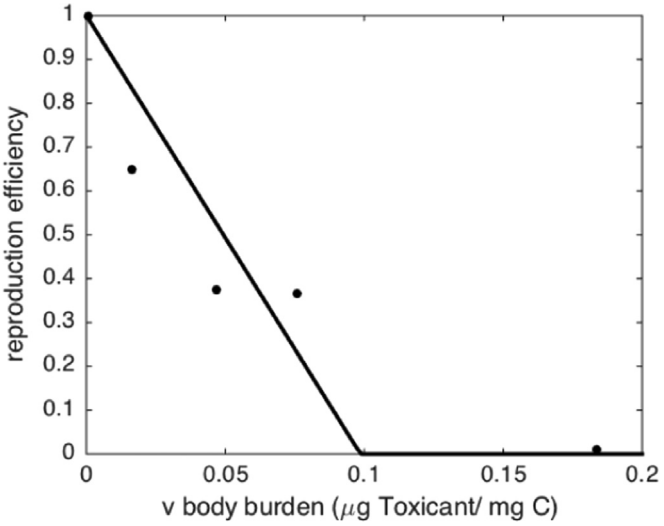

Fig. B2. Experimental data from Biesinger et al. (1982) of *Daphnia magna* exposed to MeHg for 21 days and the reproduction efficiency function (B.4) with the obtained parameter values using MATLAB's LSQCURVEFIT to fit the data.

B.3. Predator toxicant-related parameters

Tsui and Wang (2004) examined the assimilation, dissolved uptake, and efflux of Hg and MeHg in *Daphnia magna*. They report the *Daphnia* uptake coefficient for dissolved MeHg in the water is $a_2 = 0.011$ L/mg C/day. The *Daphnia* efflux rate for MeHg is $\sigma_2 = 0.04$/day and the assimilation efficiency is 0.97. Karimi et al. (2007) reported similar values for a_2 and σ_2.

B.3.1. Toxicant-dependent predator mortality rate

Here we use the power law to represent the relationship between toxicant concentrations and predator mortality rate, as recommended by the committee on toxicology of the National Research Council in 1992 and tested in Miller et al. (2000). Predator mortality rate as a function of v, the concentration of the toxicant in the predator (body burden), takes the following form:

$$d_2(v) = h_2 v^I + m_2 \tag{B.2}$$

where h_2 and I are positive constants for the coefficient and exponent of the power function and m_2 is the natural loss rate, including both natural mortality and respiration. The natural loss rate for *Daphnia* is known to be $m_2 = 0.25$/day (Andersen, 1997). To parameterize this mortality function we used data presented by Tsui and Wang (2006) on the percent survival of juvenile *Daphnia magna* after 24 h of exposure to treatments of 1.5–7 μg Hg/L. Huang et al. (2013) described the relationship between the probability of mortality after t days ($p_0(t)$) and body burden (v) as

$$p_0(t) = 1 - \exp\left(-h_2 v^I t\right). \tag{B.3}$$

Following Huang et al. (2013), we took the above mortality function (B.3) and used MATLAB's LSQCURVEFIT to fit the data presented by Tsui and Wang (2006). We obtained parameter values $h_2 = 0.347$ mg C/μg toxicant/day and $I = 1.685$. Fig. B1 shows the experimental data from Tsui and Wang (2006) and the mortality function (B.3) with the obtained parameter values. It is convenient to assume $I = 1$ for the analytical analysis presented in Section 4. Using this simplifying assumption, the mortality function (B.3) becomes $p_0(t) = 1 - \exp(-h_2 v t)$ where $h_2 = 0.0949$ mg C/μg toxicant/day when fit to the data. Fig. B1 shows this simplified mortality function with the assumption that $I = 1$ is comparable to the mortality function (B.3). In this paper, numerical simulations use the empirical mortality function parameter fits ($h_2 = 0.347$ mg C/μg toxicant/day, $I = 1.685$) and the analytical analysis assumes the simplified parameter values ($h_2 = 0.0949$ mg C/μg toxicant/day, $I = 1$).

B.3.2. Toxicant-dependent predator reproduction efficiency

We use the following linear dose response to represent the effect of the toxicant on the reproduction of the predator

$$\max\{0, 1 - \beta_2 v\} \tag{B.4}$$

which represents a linear dose response for the reproduction efficiency (Huang et al., 2013, 2014). Here we are making a simplifying assumption and only consider the effect of the toxicant on the reproduction and not on individual growth. If the predator body burden, v, reaches the threshold $\frac{1}{\beta_2}$ the reproduction efficiency is zero and reproduction ceases. To parameterize this reproduction function we used MATLAB's LSQCURVEFIT to fit the data presented by Biesinger et al. (1982) on the average number of neonates produced by *Daphnia magna* throughout 21 days of exposure to MeHg. We assumed the number of neonates produced by *Daphnia magna* in the control conditions with $v \approx 0$

represented a reproduction efficiency of 1. The reproduction efficiency for the *Daphnia magna* exposed to MeHg ($v > 0$) was calculated as the fraction of the number of neonates produced in the exposed conditions compared to the control conditions. We obtained parameter value $\beta_2 = 10.13$ mg C/μg toxicant. Fig. B2 shows the experimental data from Biesinger et al. (1982) and the reproduction efficiency function (B.4) with the fitted parameter value.

Appendix C. Algae toxicant-inhibited growth data

See Table C1.

Table C1
Relevant data from Vocke (1978) compilation of growth responses reported for freshwater algae exposed to mercury. T_0 is the reported threshold mercury concentrations that resulted in 100% growth inhibition for the various algal species. This data was used to estimate parameter α_2 using Eq. (B.1).

Algae	T_0 (mg/L)	Source
Chlamydomonas reinhardi	2	Ben-Bassat et al. (1972)
Chlorella vulgaris	0.037	de Jong and Roman (1965)
Chlorella pyrenoidosa	1	Hannan and Patouillet (1972)
Fragilaria crotonensis	1	Tompkins and Blinn (1976)

Appendix D. Proof of Theorem 4.1

Proof. First we show the solutions remain in the rectangle $\mathbf{R}$ defined by $\left[0, \mathbf{k}\right] \times \left[0, \frac{P}{\theta}\right]$, then we show solutions are also bounded by the inequality $qx + \theta y < P$. Let $S(t) = (x(t), y(t))$ be a solution of System (11) with $S(0) \in \mathbf{R}$. Assume there exists a time $t_1 > 0$ such that $S(t_1)$ touches or crosses a boundary of $\mathbf{R}$ for the first time. The following cases prove solutions remain in $\mathbf{R}$ by contradiction.

Case 1: $x(t_1) = 0$. Let $\overline{y} = \max_{t\in[0,t_1]} y(t) < \frac{P}{\theta}$. Then for every $t \in [0, t_1]$,

$$\begin{aligned}\frac{dx}{dt} &= \left(\max\left\{0, 1 - \frac{T}{\sigma_1^2}\right\}\left(1 - \frac{x}{\min\left\{K, \frac{P-\theta y}{q}\right\}}\right) - \frac{y}{a+x}\right)x \\ &\geq \left(\max\left\{0, 1 - \frac{T}{\sigma_1^2}\right\}\left(1 - \frac{x}{\min\left\{K, \frac{P-\theta \overline{y}}{q}\right\}}\right) - \frac{\overline{y}}{a+x}\right)x \\ &\geq \left(\max\left\{0, 1 - \frac{T}{\sigma_1^2}\right\}\left(1 - \frac{x}{\min\left\{K, \frac{P-\theta \overline{y}}{q}\right\}}\right) - \frac{\overline{y}}{a}\right)x \equiv \alpha x\end{aligned}$$

This implies that $x(t_1) \geq x(0)e^{\alpha t_1} > 0$, where α is a constant. This contradicts $x(t_1) = 0$ and proves that $S(t_1)$ does not reach this boundary.

Case 2: $x(t_1) = \mathbf{k} = \min\left\{K, \frac{P}{q}\right\}$. Then for every $t \in [0, t_1]$,

$$\begin{aligned}\frac{dx}{dt} &= \left(\max\left\{0, 1 - \frac{T}{\sigma_1^2}\right\}\left(1 - \frac{x}{\min\left\{K, \frac{P-\theta y}{q}\right\}}\right) - \frac{y}{a+x}\right)x \\ &\leq \max\left\{0, 1 - \frac{T}{\sigma_1^2}\right\}\left(1 - \frac{x}{\min\left\{K, \frac{P}{q}\right\}}\right)x \leq \left(1 - \frac{x}{\mathbf{k}}\right)x\end{aligned}$$

Then $x(t) < \mathbf{k}$ by a standard comparison argument. This contradicts $x(t_1) = \mathbf{k}$ and proves that the trajectory does not cross this boundary.

Case 3: $y(t_1) = 0$. Then for every $t \in [0, t_1]$,

$$\begin{aligned}\frac{dy}{dt} &= \min\left\{\beta_1, \frac{Q}{\theta}\right\}\max\left\{0, 1 - \frac{T}{\sigma_2}\left(\gamma + \frac{\beta_2}{\sigma_1^2}\frac{x}{a+x}\right)\right\}\frac{xy}{a+x} \\ &\quad - \left(\frac{h_2 T}{\sigma_2}\left(\gamma + \frac{\beta_2}{\sigma_1^2}\frac{x}{a+x}\right) + m_2\right)y \\ &\geq -\left(\frac{h_2 T}{\sigma_2}\left(\gamma + \frac{\beta_2}{\sigma_1^2}\frac{x}{a+x}\right) + m_2\right)y \\ &\geq -\left(\frac{h_2 T}{\sigma_2}\left(\gamma + \frac{\beta_2}{\sigma_1^2}\right) + m_2\right)y \equiv \alpha y\end{aligned}$$

This implies that $y(t_1) \geq y(0)e^{\alpha t_1} > 0$, where α is a constant. This contradicts $y(t_1) = 0$ and proves that $S(t_1)$ does not reach this boundary.

Case 4: $y(t_1) = \frac{P}{\theta}$. Then for every $t \in [0, t_1]$,

$$\begin{aligned}\frac{dy}{dt} &= \min\left\{\beta_1, \frac{Q}{\theta}\right\}\max\left\{0, 1 - \frac{T}{\sigma_2}\left(\gamma + \frac{\beta_2}{\sigma_1^2}\frac{x}{a+x}\right)\right\}\frac{xy}{a+x} \\ &\quad - \left(\frac{h_2 T}{\sigma_2}\left(\gamma + \frac{\beta_2}{\sigma_1^2}\frac{x}{a+x}\right) + m_2\right)y \\ &\leq \min\left\{\beta_1, \frac{Q}{\theta}\right\}\max\left\{0, 1 - \frac{T}{\sigma_2}\left(\gamma + \frac{\beta_2}{\sigma_1^2}\frac{x}{a+x}\right)\right\}\frac{xy}{a+x} \\ &\leq \frac{Q}{\theta}\max\left\{0, 1 - \frac{T}{\sigma_2}\left(\gamma + \frac{\beta_2}{\sigma_1^2}\frac{x}{a+x}\right)\right\}\frac{xy}{a+x} \leq \frac{Q}{\theta}\frac{xy}{a+x} \\ &\leq \frac{Q}{\theta}y = \left(\frac{P-\theta y}{\theta x}\right)y = \frac{xP}{\theta}\left(1 - \frac{y}{P/\theta}\right)y \leq \mathbf{k}\frac{P}{\theta}\left(1 - \frac{y}{P/\theta}\right)y\end{aligned}$$

Then $y(t) < \frac{P}{\theta}$ by a standard comparison argument. This contradicts $y(t_1) = \frac{P}{\theta}$ and proves that the trajectory does not cross this boundary. The above cases prove the trajectories are bounded in $\mathbf{R}$. Now assume $S(0) \in \Omega$ and there exists a time $t_1 > 0$ such that $S(t_1)$ touches or crosses a boundary of Ω for the first time. The final case proves solutions remain in Ω by contradiction.

Case 5: $qx(t_1) + \theta y(t_1) = P$. Then $qx(t_1) + \theta y(t_1) < P$ for every $t \in [0, t_1)$ and $qx'(t_1) + \theta y'(t_1) \geq 0$

$$\begin{aligned}x'(t_1) &= \max\left\{0, 1 - \frac{T}{\sigma_1^2}\right\}\left(1 - \frac{x(t_1)}{\min\left\{K, \frac{P-\theta y(t_1)}{q}\right\}}\right)x(t_1) - \frac{x(t_1)y(t_1)}{a+x(t_1)} \\ &\leq \max\left\{0, 1 - \frac{T}{\sigma_1^2}\right\}\left(1 - \frac{x(t_1)}{\frac{P-\theta y(t_1)}{q}}\right)x(t_1) - \frac{x(t_1)y(t_1)}{a+x(t_1)} \\ &= -\frac{x(t_1)y(t_1)}{a+x(t_1)}\end{aligned}$$

and

$$y'(t_1) = \min\left\{\beta_1, \frac{Q(t_1)}{\theta}\right\}\max\left\{0, 1 - \frac{T}{\sigma_2}\left(\gamma + \frac{\beta_2}{\sigma_1^2}\frac{x(t_1)}{a + x(t_1)}\right)\right\}$$
$$\frac{x(t_1)y(t_1)}{a + x(t_1)} - \left(\frac{h_2 T}{\sigma_2}\left(\gamma + \frac{\beta_2}{\sigma_1^2}\frac{x(t_1)}{a + x(t_1)}\right) + m_2\right)y(t_1)$$
$$\leq \frac{Q(t_1)}{\theta}\frac{x(t_1)y(t_1)}{a + x(t_1)}$$
$$= \frac{P - \theta y(t_1)}{\theta x(t_1)}\frac{x(t_1)y(t_1)}{a + x(t_1)}$$
$$= \frac{qx(t_1)}{\theta}\frac{y(t_1)}{a + x(t_1)}$$

Then $qx'(t_1) + \theta y'(t_1) \leq q\left(-\frac{x(t_1)y(t_1)}{a+x(t_1)}\right) + \theta\left(\frac{qx(t_1)}{\theta}\frac{y(t_1)}{a+x(t_1)}\right) = 0$, a contradiction. □

Appendix E. Proof of Theorem 4.2

Proof. The local stability of $E_0 = (0, 0)$ is determined by the Jacobian in the following form,

$$J(E_0) = \begin{vmatrix} \max\left\{0, 1 - \frac{T}{\sigma_1^2}\right\} & 0 \\ 0 & -\left(\frac{h_2 T\gamma}{\sigma_1^2\sigma_2} + m_2\right) \end{vmatrix}.$$

The eigenvalues have different signs, thus E_0 is a saddle point. The local stability of $E_1 = (\mathbf{k}, 0)$ is determined by the Jacobian in the following form,

$$J(E_1) = \begin{vmatrix} F(\mathbf{k}, 0) + \mathbf{k}F_x(\mathbf{k}, 0) & \mathbf{k}F_y(\mathbf{k}, 0)) \\ 0 & G(\mathbf{k}, 0) \end{vmatrix} = \begin{vmatrix} -\max\left\{0, 1 - \frac{T}{\sigma_1^2}\right\} & \mathbf{k}F_y(\mathbf{k}, 0)) \\ 0 & G(\mathbf{k}, 0) \end{vmatrix}$$

The local stability of E_1 depends on the sign of $G(\mathbf{k}, 0)$. If $G(\mathbf{k}, 0)$ is positive, then E_1 is an unstable saddle. If $G(\mathbf{k}, 0)$ is negative, then E_1 is a locally asymptotically stable node. □

References

Alexander, A.C., Luis, A.T., Culp, J.M., Baird, D.J., Cessna, A.J., 2013. Can nutrients mask community responses to insecticide mixtures? Ecotoxicology 22, 1085–1100.

Andersen, T., 1997. Pelagic Nutrient Cycles: Herbivores as Sources and Sinks. Springer-Verlag, NY.

Andersen, T., Elser, J.J., Hessen, D.O., 2004. Stoichiometry and population dynamics. Ecol. Lett. 7, 884–900.

Ankley, G.T., Erickson, R.J., Phipps, G.L., Mattson, V.R., Kosian, P.A., Sheedy, B.R., Cox, J.S., 1995. Effects of light intensity on the phototoxicity of fluoranthene to a benthic macroinvertebrate. Environ. Sci. Technol. 29, 2828–2833.

Ashauer, R., Boxall, A.B., Brown, C.D., 2007. New ecotoxicological model to simulate survival of aquatic invertebrates after exposure to fluctuating and sequential pulses of pesticides. Environ. Sci. Technol. 41, 1480–1486.

Ashauer, R., Brown, C.D., 2008. Toxicodynamic assumptions in ecotoxicological hazard models. Environ. Toxicol. Chem. 27, 1817–1821.

Ben-Bassat, D., Shelef, G., Gruner, N., Shuval, H.I., 1972. Growth of chlamydomonas in a medium containing mercury. Nature 240, 43–44.

Biesinger, K.E., Anderson, L.E., Eaton, J.G., 1982. Chronic effects of inorganic and organic mercury on *Daphnia magna*: toxicity, accumulation, and loss. Arch. Environ. Contam. Toxicol. 11, 769–774.

Bontje, D., Kooi, B., Liebig, M., Kooijman, S., 2009. Modelling long-term ecotoxicological effects on an algal population under dynamic nutrient stress. Water Res. 43, 3292–3300.

Danger, M., Maunoury-Danger, F., 2013. Ecological stoichiometry. In: Encyclopedia of Aquatic Ecotoxicology. Springer, New York, pp. 317–326.

Diehl, S., 2007. Paradoxes of enrichment: effects of increased light versus nutrient supply on pelagic producer–grazer systems. Am. Nat. 169, E173–E191.

Elser, J.J., Dobberfuhl, D.R., MacKay, N.A., Schampel, J.H., 1996. Organism size, life history, and N:P stoichiometry. BioScience 46, 674–684.

Elser, J.J., Fagan, W.F., Denno, R.F., Dobberfuhl, D.R., Folarin, A., Huberty, A., Interlandi, S., Kilham, S.S., McCauley, E., Schulz, K.L., et al., 2000. Nutritional constraints in terrestrial and freshwater food webs. Nature 408, 578–580.

Elser, J.J., Hayakawa, K., Urabe, J., 2001. Nutrient limitation reduces food quality for zooplankton: *Daphnia* response to seston phosphorus enrichment. Ecology 82, 898–903.

Elser, J.J., Urabe, J., 1999. The stoichiometry of consumer-driven nutrient recycling: theory, observations, and consequences. Ecology 80, 735–751.

Grover, J.P., 2004. Predation, competition, and nutrient recycling: a stoichiometric approach with multiple nutrients. J. Theor. Biol. 229, 31–43.

Hall, S.R., 2004. Stoichiometrically explicit competition between grazers: species replacement, coexistence, and priority effects along resource supply gradients. Am. Nat. 164, 157–172.

Hall, S.R., 2009. Stoichiometrically explicit food webs: feedbacks between resource supply, elemental constraints, and species diversity. Annu. Rev. Ecol. Evol. Syst. 40, 503–528.

Hallam, T., De Luna, J., 1984. Effects of toxicants on populations: a qualitative: approach iii. Environmental and food chain pathways. J. Theor. Biol. 109, 411–429.

Hannan, P.J., Patouillet, C., 1972. Effect of mercury on algal growth rates. Biotechnol. Bioeng. 14, 93–101.

Hansen, L.K., Frost, P.C., Larson, J.H., Metcalfe, C.D., 2008. Poor elemental food quality reduces the toxicity of fluoxetine on *Daphnia magna*. Aquat. Toxicol. 86, 99–103.

Hessen, D.O., Elser, J.J., Sterner, R.W., Urabe, J., 2013. Ecological stoichiometry: an elementary approach using basic principles. Limnol. Oceanogr. 58, 2219–2236.

Hill, W.R., Larsen, I.L., 2005. Growth dilution of metals in microalgal biofilms. Environ. Sci. Technol. 39, 1513–1518.

Huang, Q., Parshotam, L., Wang, H., Bampfylde, C., Lewis, M.A., 2013. A model for the impact of contaminants on fish population dynamics. J. Theor. Biol. 334, 71–79.

Huang, Q., Wang, H., Lewis, M., 2014. Development of a Toxin-Mediated Predator–Prey Model Applicable to Aquatic Environments in the Athabasca Oil Sands Region. OSRIN Report No. Technical Report TR-59. 59 p. ⟨http://hdl.handle.net/10402/era.40140⟩.

Huang, Q., Wang, H., Lewis, M.A., 2015. The impact of environmental toxins on predator–prey dynamics. J. Theor. Biol. 378, 12–30.

Ieromina, O., Peijnenburg, W.J., de Snoo, G., Müller, J., Knepper, T.P., Vijver, M.G., 2014. Impact of imidacloprid on *Daphnia magna* under different food quality regimes. Environ. Toxicol. Chem. 33, 621–631.

de Jong, L.d.D., Roman, W., 1965. Tolerance of Chlorella vulgaris for metallic and non-metallic ions. Antonie van Leeuwenhoek 31, 301–313.

Karimi, R., Chen, C.Y., Pickhardt, P.C., Fisher, N.S., Folt, C.L., 2007. Stoichiometric controls of mercury dilution by growth. Proc. Natl. Acad. Sci. 104, 7477–7482.

Kooijman, S., Bedaux, J., 1996. Analysis of toxicity tests on Daphnia survival and reproduction. Water Res. 30, 1711–1723.

Lessard, C.R., Frost, P.C., 2012. Phosphorus nutrition alters herbicide toxicity on *Daphnia magna*. Sci. Total Environ. 421, 124–128.

Li, X., Wang, H., Kuang, Y., 2011. Global analysis of a stoichiometric producer–grazer model with Holling type functional responses. J. Math. Biol. 63, 901–932.

Loladze, I., Kuang, Y., Elser, J., 2000. Stoichiometry in producer–grazer systems: linking energy flow with element cycling. Bull. Math. Biol. 62, 1137–1162.

Mackay, D., Puig, H., McCarty, L., 1992. An equation describing the time course and variability in uptake and toxicity of narcotic chemicals to fish. Environ. Toxicol. Chem. 11, 941–951.

McCauley, E., Nelson, W.A., Nisbet, R.M., 2008. Small-amplitude cycles emerge from stage-structured interactions in Daphnia–Algal systems. Nature 455, 1240–1243.

Mergler, D., Anderson, H.A., Chan, L.H.M., Mahaffey, K.R., Murray, M., Sakamoto, M., Stern, A.H., 2007. Methylmercury exposure and health effects in humans: a worldwide concern. AMBIO: J. Hum. Environ. 36, 3–11.

Miller, F.J., Schlosser, P.M., Janszen, D.B., 2000. Habers rule: a special case in a family of curves relating concentration and duration of exposure to a fixed level of response for a given endpoint. Toxicology 149, 21–34.

Peace, A., 2015. Effects of light, nutrients, and food chain length on trophic efficiencies in simple stoichiometric aquatic food chain models. Ecol. Model. 312, 125–135.

Peace, A., Wang, H., Kuang, Y., 2014. Dynamics of a producer–grazer model incorporating the effects of excess food nutrient content on grazers growth. Bull. Math. Biol. 76, 2175–2197.

Peace, A., Zhao, Y., Loladze, I., Elser, J.J., Kuang, Y., 2013. A stoichiometric producer–grazer model incorporating the effects of excess food-nutrient content on consumer dynamics. Math. Biosci. 244, 107–115.

Pieters, B.J., Jager, T., Kraak, M.H., Admiraal, W., 2006. Modeling responses of *Daphnia magna* to pesticide pulse exposure under varying food conditions: intrinsic versus apparent sensitivity. Ecotoxicology 15, 601–608.

Rosenzweig, M.L., et al., 1971. Paradox of enrichment: destabilization of exploitation ecosystems in ecological time. Science 171, 385–387.

Sarwar, N., Malhi, S.S., Zia, M.H., Naeem, A., Bibi, S., Farid, G., et al., 2010. Role of mineral nutrition in minimizing cadmium accumulation by plants. J. Sci. Food Agric. 90, 925–937.

Sterner, R.W., Elser, J.J., 2002. Ecological Stoichiometry: The Biology of Elements from Molecules to the Biosphere. Princeton University Press, Princeton.

Tompkins, T., Blinn, D.W., 1976. The effect of mercury on the growth rate of Fragilaria crotonensis kitton and Asterionella formosa Hass. Hydrobiologia 49, 111–116.

Tsui, M.T., Wang, W.-X., 2004. Uptake and elimination routes of inorganic mercury and methylmercury in *Daphnia magna*. Environ. Sci. Technol. 38, 808–816.

Tsui, M.T., Wang, W.-X., 2006. Acute toxicity of mercury to *Daphnia magna* under different conditions. Environ. Sci. Technol. 40, 4025–4030.

Urabe, J., Elser, J.J., Kyle, M., Yoshida, T., Sekino, T., Kawabata, Z., 2002. Herbivorous animals can mitigate unfavourable ratios of energy and material supplies by enhancing nutrient recycling. Ecol. Lett. 5, 177–185.
Urabe, J., Sterner, R.W., 1996. Regulation of herbivore growth by the balance of light and nutrients. Proc. Natl. Acad. Sci. 93, 8465–8469.
Van Voorn, G.A., Kooi, B.W., Boer, M.P., 2010. Ecological consequences of global bifurcations in some food chain models. Math. Biosci. 226, 120–133.
Vocke, R.W., 1978. Growth responses of selected freshwater algae to trace elements and scrubber ash slurry generated by coal-fired power plants. Retrospective Theses and Dissertations, Paper 6523.
Walker, C.H., Sibly, R., Hopkin, S., Peakall, D.B., 2012. Principles of Ecotoxicology. CRC Press, Boca Raton.
Wang, H., Kuang, Y., Loladze, I., 2008a. Dynamics of a mechanistically derived stoichiometric producer–grazer model. J. Biol. Dyn. 2, 286–296.
Wang, H., Sterner, R.W., Elser, J.J., 2012. On the strict homeostasis? Assumption in ecological stoichiometry. Ecol. Model. 243, 81–88.
Wang, L., Zhou, Q., Ding, L., Sun, Y., 2008b. Effect of cadmium toxicity on nitrogen metabolism in leaves of Solanum nigrum L. as a newly found cadmium hyperaccumulator. J. Hazard. Mater. 154, 818–825.
Wang, W.-X., 2012. Biodynamic understanding of mercury accumulation in marine and freshwater fish. Adv. Environ. Res. 1, 15–35.
Wang, W.-X., Fisher, N., Luoma, S., 1996. Kinetic determinations of trace element bioaccumulation in the mussel Mytilus edulis. Oceanogr. Lit. Rev. 3, 273.
Wang, W.-X., Rainbow, P.S., 2008. Comparative approaches to understand metal bioaccumulation in aquatic animals. Comp. Biochem. Physiol. Part C: Toxicol. Pharmacol. 148, 315–323.
Xie, T., Yang, X., Li, X., Wang, H., 2016. Complete global and bifurcation analysis of a stoichiometric predator–prey model. Submitted for publication.
Xing, W., Huang, W., Liu, G., 2010. Effect of excess iron and copper on physiology of aquatic plant Spirodela polyrrhiza (L.) Schleid. Environ. Toxicol. 25, 103–112.